Journal of Molecular Liquids xxx (xxxx) xxx

Contents lists available at ScienceDirect

Journal of Molecular Liquids

journal homepage: www.elsevier.com/locate/molliq

Adsorption of low molecular weight food relevant polyphenols on cross-linked agarose gel

Pamela Raquel Rivera-Tovar PhD [a,1], Javiera Pérez-Manríquez MEng [a,1], María Salomé Mariotti-Celis PhD [b], Néstor Escalona PhD [a], José Ricardo Pérez-Correa PhD [a,*]

[a] Chemical and Bioprocess Engineering Department, School of Engineering, Pontificia Universidad Católica de Chile, Vicuña Mackenna 4860, P.O. Box 306, Santiago 7820436, Chile
[b] Escuela de Nutrición y Dietética, Facultad de Medicina, Universidad Finis Terrae, Pedro de Valdivia 1509, Santiago 7501015, Chile

ARTICLE INFO

Article history:
Received 14 June 2021
Revised 19 October 2021
Accepted 25 October 2021
Available online xxxx

Keywords:
Adsorption isotherm
Adsorption thermodynamic parameters
Kaempferol
Resveratrol
Catechin
Adsorption chromatography

ABSTRACT

Adsorption of five relevant low molecular weight polyphenols identified in agro-industrial waste extracts (*Aristotelia chilensis* leaves, *Carménère* wine pomace, spent coffee grounds, and brewery waste streams) was measured and characterized. Superose^{TM} 12 prep grade and between three and six solutions with different water, ethanol, and acetic acid compositions were used as adsorbent and liquid phases. The chosen adsorbent and liquid phases were relevant for designing an adsorption preparative liquid chromatography (APLC) process to isolate these polyphenols. Langmuir and Freundlich models adequately fitted the obtained isothermal equilibrium data. The Freundlich model represented better ferulic acid (FA), kaempferol (KAE), and resveratrol (RSV) adsorptions, while the Langmuir model represented better gallic acid (GA) and catechin (CAT). Different polyphenol/agarose affinities in water-rich liquid phases were observed. From this, a hypothetical elution order was established (KAE < GA < FA < CAT < RSV), which was partially experimentally corroborated (for a mixture of GA, CAT, and RSV) with an APLC system. Lowering the water proportion or increasing the EtOH:HAc ratio in the liquid phase reduced the adsorption of these polyphenols, except for FA. The decrease in adsorption with temperature and the negative values of ΔH indicated that these processes were exothermic. The adsorption of all the polyphenols was governed by physisorption. All the adsorption processes studied were spontaneous and thermodynamically feasible ($\Delta G < 0$). In addition, the polyphenol molecules were less randomly organized (more ordered) at the polyphenol/agarose interface during the adsorption process ($\Delta S < 0$).

1. Introduction

Polyphenols (or phenolic compounds) have received particular attention as functional food ingredients and nutraceuticals due to their health-related bioactivities, including protective effects against arteriosclerosis, coronary heart disease, cancer, and many neurodegenerative diseases [1–5]. These relevant human health benefits have been ascribed to ferulic acid (FA), protocatechuic acid (PCA), gallic acid (GA), kaempferol (KAE), catechin (CAT), and resveratrol (RSV) (Fig. 1), according to many *in vitro* and *in vivo* assays [6–11]. Interestingly, these bioactive compounds can be recovered from agroindustrial wastes such as maqui leaves [12], *Carménère* wine pomace [13], spent coffee grounds [14], and brewery waste streams [15], among other sources. Many polyphenols' content is higher in these matrices than in other traditional polyphenol sources such as grape seeds, apple peel, dark chocolate, and tea leaves [12,16]. The recovery of food ingredients from agroindustrial wastes has attracted many researchers' attention because it reduces the environmental impact of this industry and increases the availability of food-relevant micronutrients such as polyphenols [17].

Consumption of diet polyphenols has been associated with several health benefits, mainly attributed to reducing the activity of free radicals. Each polyphenol presents specific properties such as antioxidant capacity, bioavailability, and solubility, as well as specific bioactivities. The desired bioactivity of a given polyphenolic natural extract can be enhanced by separating those polyphenol(s) that reduce the total antioxidant capacity of the extract (antagonistic property of some polyphenols in the mixture) [18]. Therefore, polyphenols purification is required to obtain selective natural extracts with the desired bioactive strength.

* Corresponding author.
E-mail addresses: pqrivera@uc.cl (P.R. Rivera-Tovar), jeperez1@uc.cl (J. Pérez-Manríquez), mmariotti@uft.cl (M.S. Mariotti-Celis), neescalona@ing.puc.cl (N. Escalona), perez@ing.puc.cl (J.R. Pérez-Correa).
[1] Equal contribution.

https://doi.org/10.1016/j.molliq.2021.117972
0167-7322/

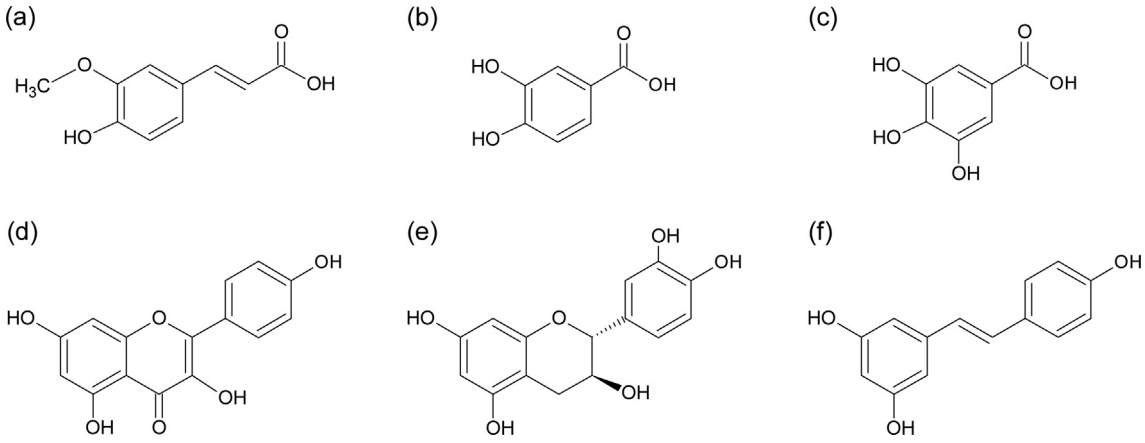

Fig. 1. Molecular structures of (a) ferulic acid, (b) protocatechuic acid, (c) gallic acid, (d) kaempferol, (e) catechin, and (f) resveratrol.

Techniques developed to isolate polyphenols generally include variations of preparative liquid chromatography, although these methods have been described as tedious, time, and solvent-consuming, as well as difficult to scale up [19–20]. Adsorption preparative liquid chromatography (APLC) with cross-linked 12% agarose gel (Superose™ 12 prep grade) has been highly recommended for polyphenols' isolation because it can be achieved in one step, and it is easily scalable to industrial size. Agarose is also stable to harsh chemical cleaning procedures [21–24]. High purities (87.2% – 99.4%) and recoveries (76.8% – 90.7%) can be obtained in step isocratic elution using mobile phases containing different proportions of water, ethanol (EtOH), and acetic acid (HAc) [21–22].

Despite the promising results obtained for polyphenol's isolation using Superose™ 12 prep grade adsorption chromatography, to our knowledge, there is no research regarding the adsorption equilibrium of polyphenols on this matrix considering mixtures of distilled water, ethanol, and acetic acid as mobile phase. This research generates preliminary information for APLC experimental optimization and scaling-up, resulting in a more efficient experimental exploration. Specifically, the estimated adsorption isotherm parameters for each polyphenol in liquid phases of different H_2O:EtOH:HAc compositions, which represent the mobile phases for polyphenols elution in APLC, are essential input data to develop predictive mathematical models of isocratic and especially gradient APLCs; these models are useful for process optimization and scaling-up [25–26]. These models typically require system parameters (e.g., porosity), mass transfer parameters (e.g., axial dispersion), and adsorption equilibrium parameters (isotherm constants), which define the elution time and consequently the polyphenols' separation [27–28]. Thus, detailed adsorption equilibrium studies are necessary to develop reliable predictive APLC models.

Langmuir and Freundlich models are widely used to represent the solid–liquid adsorption equilibrium, i.e., the relationship between the concentration of adsorbate (polyphenols for this work) in the liquid phase (H_2O:EtOH:HAc) and on the adsorbent (agarose), after reaching equilibrium at a constant temperature [29–30]. Gauss-Newton, an iterative numerical method, allows fitting experimental data to nonlinear functions, such as theoretical Langmuir and Freundlich isotherms, minimizing the weighted sum of squared errors [31]. The models and parameters fitted to these isotherms by these methods are usually adequate, accurate, and statistically significant. Additionally, from isothermal equilibrium parameters, it is possible to infer the characteristics of the adsorbent surface and information regarding each adsorbate's interaction with both phases (solution and adsorbent). The thermodynamic analysis, through the determination of enthalpy change, isosteric adsorption enthalpy change, Gibbs energy change, and entropy change, allows completing the process description since these values reveal valuable information about the process thermal nature, adsorbate-adsorbent bonding mechanism, degree of process spontaneity, and uniformity of adsorbate organization on the adsorbent surface [32–33].

This study aimed to explore and characterize the adsorption behavior of six highly bioactive polyphenols representatives of different subclasses (FA a hydroxycinnamic acid, PCA a hydroxybenzoic acid, GA a hydroxybenzoic acid, KAE a flavonol, CAT a flavanol, and RSV a stilbene) on highly cross-linked agarose. Adsorption isotherms were fitted to experimental data and then used to evaluate the effect of temperature and composition of the liquid phase (H_2O:EtOH:HAc) on each of the six studied polyphenols' adsorption capacity. The estimated isothermal equilibrium parameters are helpful to develop APLC models for process design, optimization, and scaling-up. The adsorption process was further assessed through thermodynamic analysis.

2. Materials and methods

2.1. Solvents and polyphenols standards

Ethanol (gradient grade for liquid chromatography LiChrosolv®, Merck S.A.) and glacial acetic acid (anhydrous for analysis EMPARTA® ACS, Merck S.A.) were used to prepare liquid phases where the polyphenols were dissolved. Superose™ 12 Prep Grade (GE Healthcare Lifesciences), a highly cross-linked agarose with an average particle size of 30 ± 10 μm, was used as an adsorbent. The evaluated adsorbates, ferulic acid, protocatechuic acid, gallic acid, kaempferol, catechin, and resveratrol, were purchased from Xi'an Haoxuan Bio-Tech Co., Ltd. (Baqiao, China); additional information on the chemical samples is shown in Table 1.

2.2. Batch adsorption system and experimental procedure

Adsorption isotherms were obtained using the Carousel 12 Plus™ Reaction Station (Radleys, Saffron Walden, UK) described in [34]. Adsorption experiments were performed for each polyphenol using liquids phases of different compositions (H_2O:EtOH:HAc) (Table 2). Polyphenolic solutions were prepared in the concentration ranges constrained by each compound's water solubilities (Table 2). The liquid phases used for the experiments differ between the polyphenols due to the significant differences in their

Table 1
Chemical sample description.

Sub-classes	Chemical name	CAS no.	Formula	Molar mass (g/mol)	Purity[a]
Hydroxycinnamic acid	Ferulic acid	1135–24-6	$C_{10}H_{10}O_4$	194.19	≥0.980
Hydroxybenzoic acid	Protocatechuic acidGallic acid	99–50-3149–91-7	$C_7H_6O_4C_7H_6O_5$	154.12170.12	≥0.990
Hydrobenzoic acid	Gallic acid	149-91-7	$C_7H_6O_5$	170.12	≥0.990
Flavonol	Kaempferol	520–18-3	$C_{15}H_{10}O_6$	286.24	≥0.980
Flavanol	Catechin	154–23-4	$C_{15}H_{14}O_6$	290.26	≥0.980
Stilbene	Resveratrol	501–36-0	$C_{14}H_{12}O_3$	228.25	≥0.980
	Ethanol	64–17-5	C_2H_6O	46.07	≥0.999
	Acetic acid	64–19-7	$C_2H_4O_2$	60.05	≥0.997

[a] Informed by the corresponding chemical suppliers.

Table 2
Some specifications for adsorption experiments: water solubility, concentration range of polyphenolic solutions, liquid phase composition, and absorbance reading.

Compound	Water solubility[a] (mg/L water) at 20 to 25 °C	Polyphenol concentration range (mmol/L liquid phase)	Liquid phase composition (H_2O:EtOH:HAc v/v)	Maximum wavelength (nm)
FA	524.8 [35] 527.0 [36]	0.515–2.575 (100–500)[b]	90:5:5 (W90) 70:15:15 (W70) 50:25:25 (W50) 30:35:35 (W30)	325
PCA	18,521 [37] 29,400 [38]	6.488–38.931 (1000–6000)[b]	100:0:0 (W100) 70:15:15 (W70) 50:25:25 (W50) 30:35:35 (W30)	260
GA	9583 [39] 14,940 [40]	7.054–35.269 (1200–6000)[b]	100:0:0 (W100) 94:3:3 (W94) 80:10:10 (W80) 70:15:15 (W70) 30:35:35 (W30)	260 270
KAE	1.25 [41] 1.34 [42]	0.028–0.168 (8–48)[b]	70:15:15 (W70) 50:25:25 (W50) 30:35:35 (W30)	265
CAT	4544 [34] 7620 [43]	2.412–14.470 (700–4200)[b]	100:0:0 (W100) 94:3:3 (W94) 80:10:10 (W80) 70:15:15 (W70) 50:25:25 (W50) 30:35:35 (W30)	275
RSV	24.15 [44] 50.00 [45]	0.035–0.210 (8–48)[b]	100:0:0 (W100) 94:3:3 (W94) 80:10:10 (W80) 70:15:15 (W70) 30:35:35 (W30)	305

[a] values used as a reference in the definition of maximum concentrations of each polyphenol. [b] equivalent values in mg/L.

solubilities. Isotherm curves were set up using 5 or 6 different initial concentrations of each polyphenol.

In the adsorption experiments, 0.005 g dry weight of cross-linked 12% agarose was weighed (previously washed with distilled water to displace the storage ethanol, moisture: 86.1%) in an analytical balance with a resolution of 0.0001 g and then added to the glass tubes inside the Carrousel. Once the Carrousel system reached a temperature of 20 °C, 0.005 L of the polyphenolic solutions (at 20 °C) were poured into the corresponding flask. All glass tubes were carefully capped to avoid evaporation. The solution-adsorbent mixture was kept under agitation (500 rpm) at 20 °C for 60 min (allowing equilibrium). Adsorption experiments were previously followed for 6 h to define the equilibrium time. A significant change in the liquid phase polyphenol concentration was observed during the first minutes (~5 min) and then remained practically invariant (Fig. 1**S**). Once the adsorption equilibrium was reached, the liquid and solid phases were quickly separated using a polytetrafluoroethylene (PTFE) syringe filter with a pore size of 0.45 μm and a diameter of 13 mm (Bonna-Agela Technologies, Delaware, USA). The filtrates were diluted, so polyphenol concentrations could be measured using an ultraviolet–visible spectrophotometer (Reyleigh UV-1601, Beijing Beifen-Ruili Analytical Instrument Co. Ltd., Beijing, China). Each polyphenol's absorbance was measured within the range of 200–600 nm to establish the maximum wavelengths for spectrophotometric measurements (Table 2).

A similar procedure was carried out to assess the effect of temperature in polyphenols adsorption from a liquid phase (W70, Table 2). In this case, the experiments were performed at 10 °C and 30 °C, keeping the rest of the operating conditions invariable.

Calibration curves (R^2 > 0.997) for each polyphenol in each liquid phase were prepared to correlate absorbance and concentration. Increases in concentration during absorbance determination due to evaporation were prevented by using cell caps. After the concentration of the polyphenolic solutions was calculated, C_e (mmol/L), the equilibrium adsorption capacity, q_e (mmol/g), was calculated using a mass balance,

$$q_e = (C_0 - C_e) \cdot V/m_A \quad (1)$$

where V is the volume of the polyphenolic solution (L), m_A is the dry weight of agarose (g), and C_0 is the concentration of the solution before the adsorption process (mmol/L).

2.3. Fitting of adsorption isotherm models

The adsorption isotherms describe the relationship between the amount of polyphenol adsorbed on agarose (q_e, mmol/g) and the polyphenol diluted in the liquid phase (C_e, mmol/mL) at equilibrium. The most commonly used isotherm models, Langmuir and Freundlich, were applied in our study to find which one represents better the adsorption process of the studied system (polyphenol-agarose-liquid phase). The Langmuir model assumes monolayer adsorption and a fixed number of adsorption sites. It also assumes that all adsorption sites are equal, and there is no interaction between adsorbed molecules [46]. This model can be described as:

$$q_e = q_{max} K_L C_e / (1 + K_L C_e) \tag{2}$$

where q_{max} (mmol/g) is the maximum adsorption capacity and K_L (L/mmol) is the adsorption equilibrium constant.

The Freundlich model is often used to represent non-ideal adsorption. It is characterized by multilayer formation, heterogeneous surface, and irregular heat adsorption distributions [47]. The equation that describes the Freundlich isotherm is:

$$q_e = K_F C_e^{1/n} \tag{3}$$

where K_F (mmol/g)(L/mmol)$^{1/n}$ and n are model parameters associated with adsorption capacity of the adsorbent and adsorption intensity or degree of surface heterogeneity, respectively [46].

Model parameters were estimated through nonlinear weighted regression where the weighted sum of the squares of the distances of the data points to the modeled curve (WSSE) Eq. (4) was minimized by Minitab® Statistical Software v.19 using a Gauss-Newton iterative algorithm (maximum number of iterations: 200 and convergence tolerance: 0.00001). Initial values of the parameters that allowed convergence to the minimum values were: [0.1 0.1] and [1 1] for Langmuir and Freundlich parameters, respectively.

$$WSSE = \sum_{i=1}^{N} w_i \left(q_{calc} - q_{exp}\right)_i^2 \tag{4}$$

where q_{calc} is the adsorbed polyphenol value calculated by the model, q_{exp} is the experimental measurement of the adsorbed polyphenol, N represents the number of data points, and w_i is the weight assigned to each observed point. The reciprocal coefficient of variation (CV) of each observation's replications is generally considered an appropriate weight because observations with small experimental errors weigh more, and observations with large experimental errors weigh less; this compensates for the heteroscedasticity of the residuals.

Discrimination between Langmuir and Freundlich fitted models for each case was carried out according to several criteria. Three of them referred to the residuals: the standard regression error (S, Eq. (5)), the coefficient of determination (R^2, Eq. (6)) and residual plots; and three other criteria referred to the estimated parameters: correlation matrix (C, Eq. (7)), confidence intervals (CI, Eq. (8)) and confidence coefficient (CC, Eq. (9)). Although these criteria were defined for linear functions, which underestimate the nonlinear equation's true uncertainty, they can be useful and accepted as a valid approximation if interpreted correctly.

S is measured in the units of the response variable and represents how far the data values fall from the fitted values,

$$S = \sqrt{WSSE/(N-p)} \tag{5}$$

p is the number of model parameters.

R^2 represents the ratio between the explained variance and the total variance,

$$R^2 = 1 - \frac{WSSE}{SST} = 1 - \frac{\sum_{i=1}^{N} w_i \left(q_{calc} - q_{exp}\right)^2}{\sum_{i=1}^{N} \left(q_{exp} - \bar{q}_{exp}\right)^2} \tag{6}$$

$\bar{q}_{exp}$ is the mean of the experimental values of the adsorbed polyphenol.

The correlation matrix of the parameter estimates (C) was used to identify those parameters that were strongly correlated ($|C_{pq}| > 0.99$). Matrix C was calculated by Minitab® Statistical Software v.19 based on the approximate variance–covariance matrix of the parameter estimates:

$$C = S^2 \left(R' R\right)^{-1} = R^{-1} \left(R^{-1}\right)' \tag{7}$$

The approximate correlation between the estimates of θ_p and θ_q is:

$$\left(C_{pq}\right) / \left(\sqrt{C_{pp} C_{qq}}\right)$$

R is the (upper triangular) matrix from the QR decomposition of the Jacobian evaluated at θ^i (parameter estimate after iteration i) for the final iteration. θ_p and θ_q represent the two estimated parameters of each model.

CI defines the range of values that are likely to contain the true value of the model parameter (95% confidence). The function *nlparci* of MATLAB v. R2019a was used to determine the confidence intervals based on the variability observed in the sample, the sample size, and the confidence level.

$$CI = \theta \pm \sigma \cdot t_{\alpha/2} \tag{8}$$

σ is the standard deviation of the estimated parameter (variance–covariance matrix function), and $t_{\alpha/2}$ is the upper point of the Student's t distribution with N-p degrees of freedom.

CC was calculated according to [48]. A parameter was considered statistically significant (different from zero) when the following criterion was fulfilled:

$$CC = \Delta(CI)/\theta < 2 \tag{9}$$

$\Delta(CI)$ is the width of the confidence intervals.

2.4. Thermodynamic analysis

Further understanding of the adsorption process can be attained through thermodynamic analysis. The enthalpy change (ΔH, kJ/mol), Gibbs free surface energy change (ΔG, kJ/mol), and the entropy change (ΔS, kJ/mol K) can provide information related to the energy changes that occurred on agarose after adsorption and the mechanisms involved in this process [32]. The spontaneity of the system was determined by evaluating ΔG at equilibrium conditions, as was done for the solid–liquid adsorption of polyphenols from *Eucommia ulmoides* oliv. leaves on macroporous resin [49], sulforaphane on macroporous resin [50], polyphenols on eucalyptus bark powders [51], and cadmium on orange peel [33]:

$$\Delta G = -RT \ln K_{eq} \tag{10}$$

where T is the absolute temperature (K), R is the ideal gas constant (8.314 J/mol K), and K_{eq} is the thermodynamic equilibrium constant (dimensionless), which was calculated from the distribution coefficient, K_d (L/g), by plotting $\ln(q_e/C_e)$ versus C_e and extrapolating to zero [33]. To achieve a dimensionless constant, K_d was multiplied by the $\rho(T)$ of the liquid phase (H_2O:EtOH:HAc), as proposed by Milonjić [52]. The ΔH and ΔS values were determined by plotting $\ln K_{eq}$ against $1/T$ (the van't Hoff equation, Eq. (11)) and multiplying the slope and the intercept by R.

$$\ln K_{eq} = -\frac{\Delta H}{R}\frac{1}{T} + \frac{\Delta S}{R} \tag{11}$$

This well-known equation is obtained by substituting Eq. (10) into the Gibbs-Helmholz (Eq. (12)) equation and the fundamental relation between ΔG, ΔH, *and* ΔS (Eq. (13)).

$$\left(\frac{\partial \frac{\Delta G}{T}}{\partial T}\right)_P = -\frac{\Delta H}{T^2} \quad (12)$$

$$\Delta G = \Delta H - T\Delta S \quad (13)$$

The enthalpy change of adsorption at a constant amount of adsorbed adsorbate is defined as the isosteric adsorption enthalpy change (ΔH_x, kJ/mol). This important thermodynamic parameter indicates the adsorption performance and the surface energy heterogeneity [53]. The isosteric adsorption enthalpy change with a constant surface coverage is obtained from the integrated Clausius-Clapeyron equation and assuming that ΔH_x is independent of temperature, as follows:

$$\ln C_e = \frac{\Delta H_x}{R}\frac{1}{T} + K \quad (14)$$

where K is an integration constant. ΔH_x can be determined from the slope of the isosteres, plot of ln C_e versus $1/T$. The different equilibrium concentrations (C_e) of the isosteres were obtained at a constant adsorbed amount (q) at three temperatures.

Each parameter is presented with the corresponding combined standard uncertainty (U) calculated as described in [54].

2.5. Statistical analysis

All the adsorptions and chemical analyses were performed in triplicate (in some cases, additional repetitions were performed). Experimental values obtained were presented as means ± SD, and estimated parameters were presented with uncertainties. Statistical analysis was carried out using Minitab® Statistical Software v.19 and MATLAB v. R2019a.

2.6. Three-component mixing experiments in APLC system

Additionally, experiments in the BioLogic DuoFlow™ Chromatography System (Bio-Rad) were carried out to contrast the elution order defined according to the adsorption affinities of each polyphenol with the Superose™ 12. An aqueous mixture of gallic acid, catechin, and resveratrol was prepared, which contained 1, 0.5, and 1.5 g/L, respectively. An Econo-Column (1x10 cm) was packed with Superose™ 12 [55]. Two mobile phases were assessed (W94 and W70, Table 2), which were pumped isocratically. The mixture was injected into the system (0.2 mL) and eluted with a 1 mL/min mobile phase flowrate. The effluent was monitored at three wavelengths simultaneously (270, 275, and 305, Table 2).

3. Results and discussion

3.1. Experimental adsorption isotherms

Adsorption isotherms of six polyphenols (FA, PCA, GA, KAE, CAT, RSV) on agarose considering liquid phases with different compositions (H_2O:EtOH:HAc) at 20 °C were studied; the experimental curves are presented in Fig. 2. According to the isotherm classification system defined by Giles & Smith [56], based on the initial slope form, all our curves followed the L-type shape, indicating that as more sites on agarose are filled in, it becomes much more difficult for a polyphenol molecule to find a vacant site. Also, polyphenols are either horizontally adsorbed or show no strong competition from the liquid phase.

The obtained isotherms show different shapes past the origin (a subgroup of the Giles classification). The FA curves exhibit subgroup L1 shapes due to the absence of an inflection point. This absence means these curves are incomplete, probably because FA initial concentrations in the liquid phases were not high enough. Nevertheless, these high concentrations are not relevant for the current study since they have not been found in natural sources. Whereas GA, KAE, CAT, and RSV curves show subgroup L2 shapes, having an inflection point, an apparent plateau (e.g., GA - W30), a slight change in slope post the inflection point (e.g., CAT - W94), or a continually rising curve (e.g., KAE - W50). Finally, PCA curves present L4 shapes that are characterized by a second rise and a second plateau. This behavior could have appeared due to a re-orientation of the adsorbed PCA molecules (horizontal orientation at the first plateau and vertical orientation at the second) or because a second layer has been formed [56]. PCA curves did not agree with the theoretical isotherm models evaluated in this study. Consequently, this polyphenol was not considered in the subsequent analyzes. PCA isotherms could be analyzed by increasing the number of observations in the first rise and considering only this region; the second rise contains exceptionally high concentrations not found in natural matrices.

The effect of the liquid phase composition on the adsorption capacity was the same for all the polyphenols analyzed (Fig. 3). At high water concentrations (W100 for GA, CAT, and RSV; W90 for FA; and W70 for KAE), the highest adsorption capacities were observed, which decreased (in different proportions for each polyphenol) with decreasing concentrations of water. RSV's mean maximum adsorption reached 93.6%, which was the highest of the polyphenols evaluated here, followed by CAT (13.3%), FA (4.5%), GA (3.1%), and finally KAE (2.8%). These results show the high affinity of RSV with agarose, which in chromatography translates into a problematic elution that must necessarily be accelerated with the decrease in water concentration in the mobile phase [57]. On the other hand, GA or KAE, showing the lowest affinities for agarose, would elute more efficiently, even with a liquid phase with high water concentrations. This behavior was observed by Tan et al. [58], who found that GA eluted at ~ 170 min with a mobile phase of 5% EtOH and 5% HAc (W90) while RSV elution required a gradient in the mobile phase with 30% EtOH and 30% HAc (W40) as the final mobile phase at ~ 321 min.

The average adsorptions of GA, CAT, and RSV with the W70 liquid phase were 0.8%, 2.6%, and 1.4%, respectively. The change from W100 to W70 generated a more significant impact on RSV adsorption (reduced ~ 59 times) followed by CAT adsorption (reduced ~ 5 times) and GA adsorption (reduced ~ 3 times). Similarly, the change from W70 to W30 generated more similar reductions on the adsorptions of five polyphenols (~2–3 times less). With W30 liquid phase, most polyphenols (safe FA with 2.8%) only reached an average adsorption of ~ 0.9%. Due to these low adsorptions, W30 (or solutions with even less water) is an excellent mobile phase to elute these polyphenols in APLC. The adsorption capacities of FA were similar with W30, W50, and W70; these liquid phases reduced ~ 2 times the average maximum adsorption (4.5%).

The adsorption behavior against changes in liquid phase composition (decrease in water) can be attributed to polyphenols solvophobicity. A greater polyphenol solvophobicity in a specific liquid phase means a stronger tendency of liquid phase molecules to push polyphenol molecules towards agarose. Silva et al. [59] observed high polyphenol solvophobicities in liquid phases with high dielectric constants (water, ε_{H2O} = 78.5) and low solvophobicities in liquid phases with low dielectric constants (ethanol and acetic acid, ε_{EtOH} = 24.3 and ε_{HAc} = 6.15). The liquid phase pH can also affect the adsorption process, accelerating or delaying the fractions elution in an APLC system. High acetic acid concentrations in the liquid phase could be responsible for adsorption reduction since it reduces the available sites for polyphenols adsorption. Interaction of acetate ions and delocalized electrons from the agarose surface could also influence the process [20]. However, the addition of EtOH:HAc in fixed proportions generated liquid phases without significant differences in their pHs, which reached values

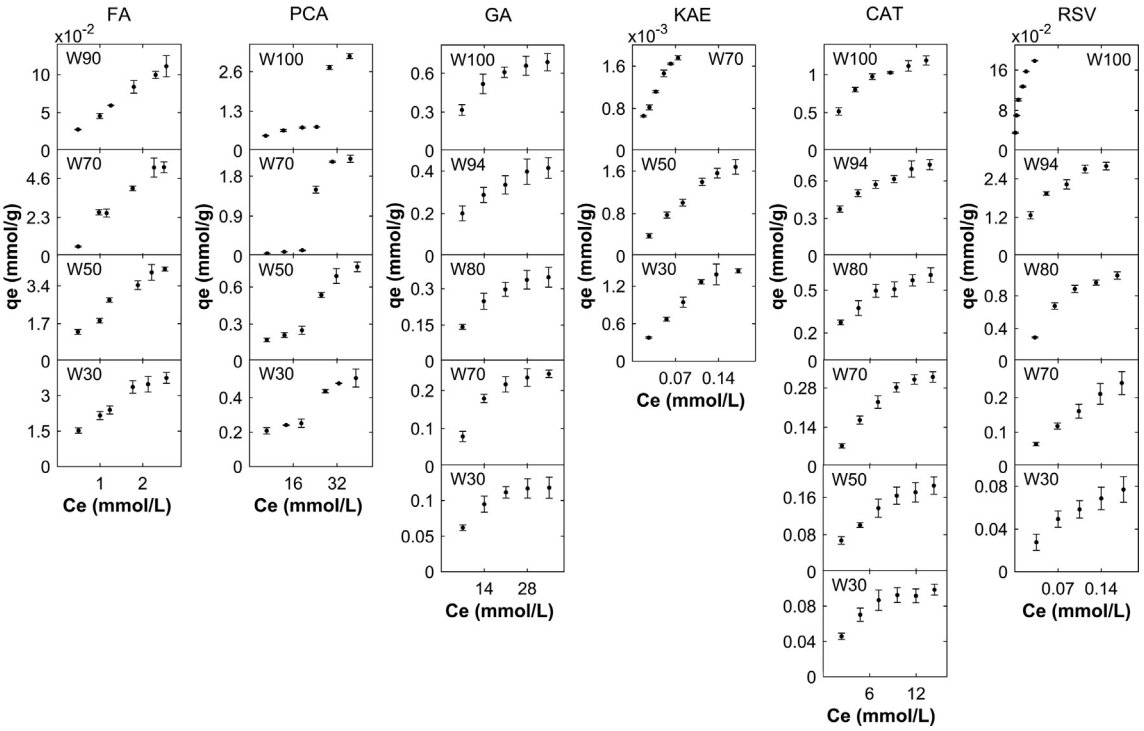

Fig. 2. Equilibrium experimental data of the six polyphenols evaluated in 3–6 liquid phases with different compositions (W100, W94, W90, W80, W70, W50, and W30) at 20 °C. Each column corresponds to a given polyphenol: FA (ferulic acid), PCA (protocatechuic acid), GA (gallic acid), KAE (kaempferol), CAT (catechin), and RSV (resveratrol).

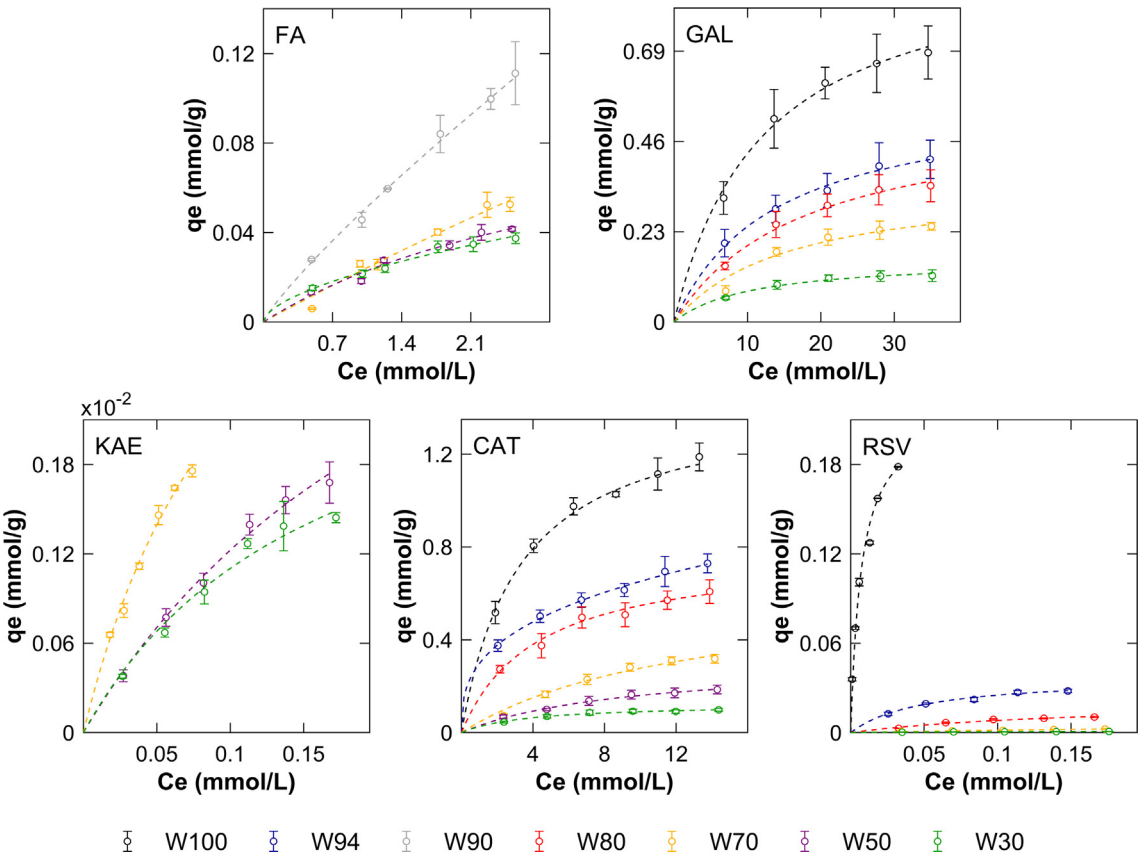

Fig. 3. Effect of liquid phase composition (W100, W94, W90, W80, W70, W50, W30, and W90; see Table 2) on polyphenol adsorption for the five studied polyphenols: FA (ferulic acid), GA (gallic acid), KAE (kaempferol), CAT (catechin) and RSV (resveratrol). This effect for the first plateau of PCA is shown in Fig. 2**S**.

Table 3
Estimated parameters and the goodness-of-fit of Langmuir and Freundlich models.

Compound, liquid phase/T (°C)		Langmuir model					Freundlich model				
		q_{max} (CC)	K_L (CC)	S (S%)	R^2	|C|	K_F (CC)	n (CC)	S (S%)	R^2	|C|
FA	W90/20	4.98E-01 (1.22)	1.09E-01 (1.42)	1.23E-03 (2.0)	0.9992	0.9988[b]	4.93E-02 (0.06)	1.17E+00 (0.14)	9.86E-04 (1.6)	0.9996	0.7291
	W70/20	5.59E-01 (8.87)[a]	4.32E-02 (9.63)[a]	1.33E-03 (4.6)	0.9967	0.9998[b]	2.27E-02 (0.43)	1.03E+00 (0.61)	1.52E-03 (5.3)	0.9965	0.8990
	W50/20	1.02E-01 (1.10)	2.77E-01 (1.71)	8.79E-04 (3.5)	0.9972	0.9941[b]	2.20E-02 (0.28)	1.43E+00 (0.51)	1.02E-03 (4.1)	0.9970	0.8976
	W30/20	6.63E-02 (0.61)	5.17E-01 (1.15)	5.49E-04 (2.3)	0.9986	0.9837	2.23E-02 (0.17)	1.73E+00 (0.42)	5.75E-04 (2.4)	0.9987	0.8081
	W70/10	2.01E-01 (0.40)	2.64E-01 (0.62)	9.03E-04 (1.9)	0.9992	0.9934[b]	4.09E-02 (0.10)	1.36E+00 (0.17)	1.10E-03 (2.3)	0.9991	0.8711
	W70/30	7.24E-02 (1.58)	2.10E-01 (2.04)	1.35E-03 (9.1)	0.9828	0.9947[b]	1.22E-02 (0.36)	1.26E+00 (0.59)	1.83E-03 (10.1)	0.9747	0.8378
GA	W100/20	9.44E-01 (0.26)	8.35E-02 (0.73)	5.13E-03 (1.1)	0.9997	0.9642	1.67E-01 (1.10)	2.42E+00 (0.84)	1.26E-02 (2.7)	0.9986	0.9909[b]
	W94/20	5.77E-01 (0.25)	7.30E-02 (0.65)	2.45E-03 (0.9)	0.9998	0.9652	9.02E-02 (0.48)	2.30E+00 (0.35)	2.87E-03 (1.1)	0.9998	0.9903[b]
	W80/20	5.41E-01 (0.36)	5.62E-02 (0.79)	3.08E-03 (1.3)	0.9996	0.9689	5.83E-02 (1.11)	1.93E+00 (0.67)	6.78E-03 (3.0)	0.9985	0.9881
	W70/20	3.58E-01 (0.63)	6.47E-02 (1.64)	4.82E-03 (3.0)	0.9981	0.9707	5.15E-02 (1.76)	2.24E+00 (1.20)	7.79E-03 (4.9)	0.9962	0.9926[b]
	W30/20	1.60E-01 (0.31)	9.62-E02 (0.88)	1.32E-03 (1.6)	0.9993	0.9479	3.13E-02 (1.09)	2.53E+00 (0.90)	2.77E-03 (3.3)	0.9978	0.9860
	W70/10	6.56E-01 (0.30)	3.98E-02 (0.55)	2.95E-03 (1.3)	0.9997	0.9791	4.71E-02 (0.90)	1.68E+00 (0.48)	7.93E-03 (3.4)	0.9982	0.9878
	W70/30	2.30E-01 (0.40)	3.78E-02 (0.76)	9.00E-04 (1.1)	0.9997	0.9847	1.71E-02 (0.98)	1.73E+00 (0.52)	1.81E-03 (2.3)	0.9992	0.9922[b]
KAE	W70/20	4.54E-03 (0.66)	8.87E+00 (0.99)	2.76E-05 (2.6)	0.9984	0.9958[b]	1.20E-02 (0.65)	1.38E+00 (0.31)	3.63E-05 (3.4)	0.9977	0.9941[b]
	W50/20	4.61E-03 (0.88)	3.62E+00 (1.27)	1.84E-05 (1.9)	0.9993	0.9959[b]	6.79E-03 (0.67)	1.33E+00 (0.42)	2.75E-05 (2.8)	0.9987	0.9871
	W30/20	2.90E-03 (0.77)	6.12E+00 (1.36)	3.29E-05 (3.8)	0.9970	0.9871	4.81E-03 (0.85)	1.53E+00 (0.62)	5.15E-05 (5.9)	0.9941	0.9793
	W70/10	5.69E-03 (0.64)	7.06E+00 (0.90)	3.74E-05 (3.2)	0.9977	0.9968[b]	1.34E-02 (0.53)	1.36E+00 (0.25)	4.58E-05 (3.9)	0.9972	0.9944[b]
	W70/30	5.25E-03 (1.32)	6.15E+00 (1.72)	5.39E-05 (5.7)	0.9931	0.9967[b]	1.31E-02 (1.06)	1.26E+00 (0.44)	7.31E-05 (7.7)	0.9898	0.9926[b]
CAT	W100/20	1.44E+00 (0.17)	3.05E-01 (0.57)	1.20E-02 (1.5)	0.9993	0.9645	4.83E-01 (0.39)	2.83E+00 (0.52)	2.07E-02 (2.6)	0.9984	0.9839
	W94/20	8.52E-01 (0.25)	3.37E-01 (0.87)	1.05E-02 (2.1)	0.9985	0.9350	2.98E-01 (0.16)	2.94E+00 (0.22)	5.02E-03 (1.0)	0.9997	0.9718
	W80/20	7.77E-01 (0.22)	2.39E-01 (0.65)	5.88E-03 (1.5)	0.9994	0.9427	2.06E-01 (0.36)	2.40E+00 (0.39)	7.47E-03 (1.8)	0.9992	0.9725
	W70/20	6.38E-01 (0.76)	7.71E-02 (1.38)	5.08E-03 (2.6)	0.9986	0.9897	6.21E-02 (1.06)	1.56E+00 (0.69)	8.30E-03 (4.2)	0.9970	0.9885
	W50/20	3.08E-01 (0.35)	1.08E-01 (0.68)	1.57E-03 (1.3)	0.9995	0.9772	4.37E-02 (0.47)	1.80E+00 (0.37)	2.30E-03 (2.0)	0.9992	0.9784
	W30/20	1.25E-01 (0.21)	2.63E-01 (0.66)	9.67E-04 (1.4)	0.9994	0.9371	3.75E-02 (0.61)	2.68E+00 (0.70)	2.00E-03 (2.9)	0.9979	0.9755
	W70/10	7.26E-01 (0.47)	1.15E-01 (0.90)	5.51E-03 (2.0)	0.9990	0.9802	1.05E-01 (0.70)	1.78E+00 (0.58)	9.68E-03 (3.5)	0.9976	0.9772
	W70/30	4.02E-01 (0.63)	8.63E-02 (1.12)	2.64E-03 (2.0)	0.9991	0.9834	4.18E-02 (0.84)	1.56E+00 (0.58)	4.59E-03 (3.4)	0.9978	0.9770
RSV	W100/20	2.17E-01 (0.19)	1.40E+02 (0.72)	7.00E-03 (7.3)	0.9902	0.9609	5.83E-01 (0.88)	2.97E+00 (0.68)	8.58E-03 (9.0)	0.9883	0.9816
	W94/20	3.74E-02 (0.28)	2.05E+01 (0.77)	3.54E-03 (1.9)	0.9991	0.9556	6.14E-02 (0.56)	2.52E+00 (0.58)	5.54E-04 (3.0)	0.9983	0.9799
	W80/20	2.15E-02 (1.24)	6.18E+00 (2.03)	3.18E-04 (4.9)	0.9953	0.9874	3.75E-02 (1.31)	1.48E+00 (0.89)	4.86E-04 (7.5)	0.9918	0.9801
	W70/20	8.32E-03 (0.58)	2.39E+00 (0.75)	9.20E-06 (0.7)	0.9999	0.9967[b]	1.02E-02 (0.26)	1.23E+00 (0.15)	1.13E-05 (0.9)	0.9999	0.9807
	W30/20	1.29E-03 (0.21)	8.26E+00 (0.69)	3.70E-06 (0.8)	0.9999	0.9842	2.05E-03 (0.49)	1.80E+00 (0.41)	6.10E-06 (1.4)	0.9997	0.9836
	W70/10	7.47E-03 (0.21)	4.40E+00 (0.32)	9.70E-06 (0.5)	0.9999	0.9911[b]	1.18E-02 (0.45)	1.38E+00 (0.27)	3.65E-05 (2.0)	0.9994	0.9782
	W70/30	3.02E-03 (0.14)	5.43E+00 (0.22)	2.60E-06 (0.3)	1.0000	0.9891	4.79E-03 (0.40)	1.51E+00 (0.27)	1.14E-05 (1.3)	0.9997	0.9813

[a] statistically non-significant parameter.
[b] Highly correlated parameters.

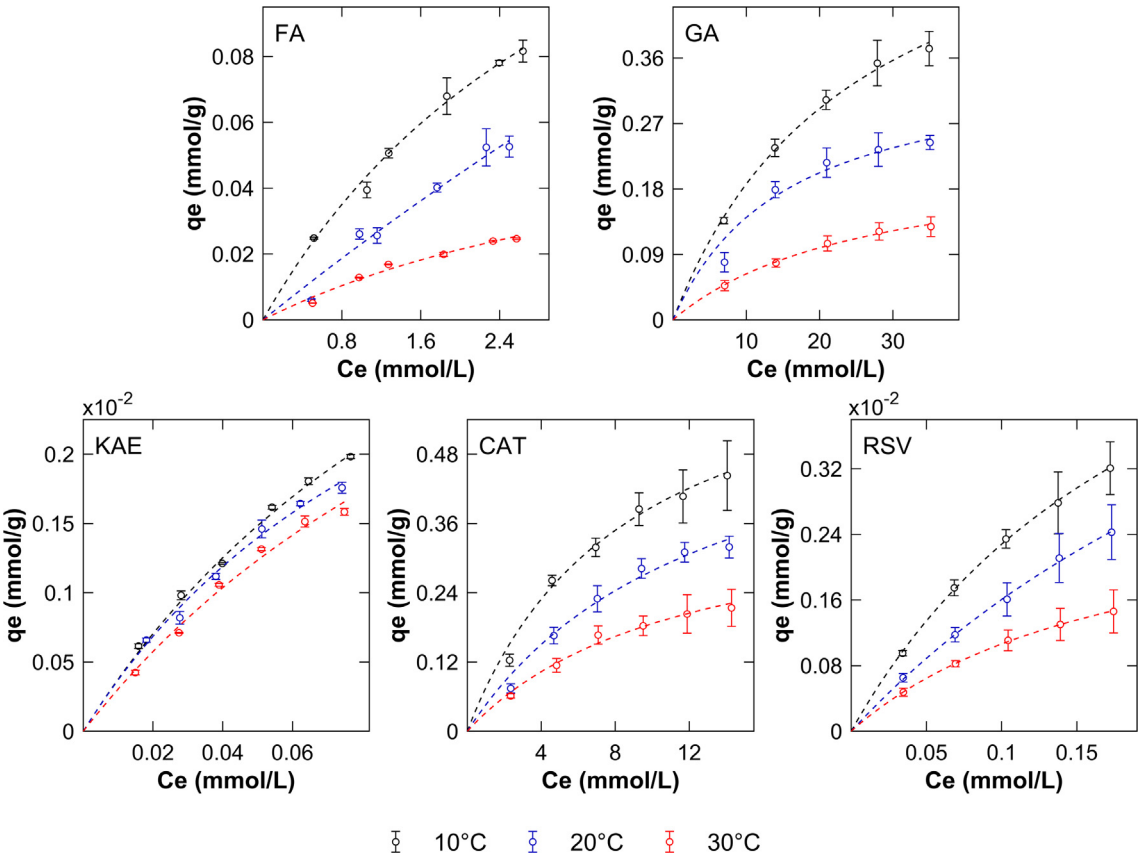

Fig. 4. Temperature effect on polyphenols adsorption on agarose from W70 liquid phase for FA (ferulic acid), GA (gallic acid), KAE (kaempferol), CAT (catechin), and RSV (resveratrol). This effect for the first plateau of PCA is shown in Fig. 2**S**.

of 2.66 (W94), 2.57 (W90), 2.42 (W80), 2.33 (W70), 2.18 (W50), and 2.05 (W30). Only the liquid phase of pure water (W100) had a difference in pH, whose value was 6.30.

Although there are several interactions of different physical nature between the molecules of the solute and the phases (size exclusion, ion exchange, reverse phase, adsorption, and others), which generate the delay of the solutes in the APLC, the adsorption equilibrium isotherm is an adequate approximation to quantify this phenomenon [28]. Superose^{TM} 12 gel medium has been widely used to isolate large biomolecules such as proteins by size exclusion chromatography processes [60]. However, in our case, this interaction could be ignored because the Mr range of the polyphenols (170–290) was well below the optimal separation range (Mr 1000–300000) offered by the Superose^{TM} 12 [55]. Therefore it can be considered that for these polyphenols, the size exclusion is too weak to affect the fractions delay.

Contrarily, the number of OH in the polyphenol molecular structure delays its elution since this functional group forms hydrogen bonds between the polyphenol and the Superose^{TM} 12. Then, the higher the number of OH, the stronger the retention [61]. However, this relationship is often not so direct since the OH's position in the aglycone's molecular structure also affects retention. The molecular structures in which the OHs are distant generate higher retention in the resin because these structures favor hydrogen bonding with the Superose. In contrast, molecular structures with their OHs closest to each other could form intramolecular hydrogen bonds, as proposed for gallic acid [20]. Consequently, the spatial positions of this functional group on the polyphenol structure must also be considered. Therefore, the order of elution based on the number and position of the OH could be: KAE and GA (4 OH) < FA (2 OH, one of them distant from the benzene ring) < CAT (5 OH) < RSV (3 OH, 2 benzene rings apart) (Fig. 1), which is consistent with the average adsorption percentage. It can be seen that FA is more strongly retained than KAE and GA that have more OH in their structures due to the spatial position of its OH. The same behavior is observed when CAT and RSV are compared.

3.2. Models fitting

The estimated isothermal equilibrium parameters and the goodness of fit statistics obtained by nonlinear weighted regression of Langmuir and Freundlich models for each isotherm (33 total) are presented in Table 3.

R^2 values ranged between 0.9828 and 1.0000 for Langmuir and between 0.9747 and 0.9999 for Freundlich. *S* values for both models were low; they represented<10.0% of the mean of the endogenous variable (q_e). Together with residual plots, these results indicate that both isotherm models fitted correctly to all experimental curves and were adequate models because their residuals were independent and normally distributed. In most cases, except for FA-W90, FA-W30, and CAT-W94, Langmuir fitted models achieved a slightly higher R^2 and a slightly lower S than Freundlich fitted models. However, these statistics were not discriminant enough to choose Langmuir as the best model, given the minor differences in their values (ΔR^2_{max} = 0.0081 and ΔS_{max} = 3.2%).

Statistical criteria referring to estimated parameters (*CI, CC, and* |*C*|) provided additional information to choose the best-fit model. The fitted parameters of both models for the studied polyphenols were statistically significant (*CC* < 2), except those of FA-W70-20 °C of the Langmuir model, whose *CC*s were high (8.87 for q_{max} and 9.63 for K_L) respectively. Freundlich parameters were more

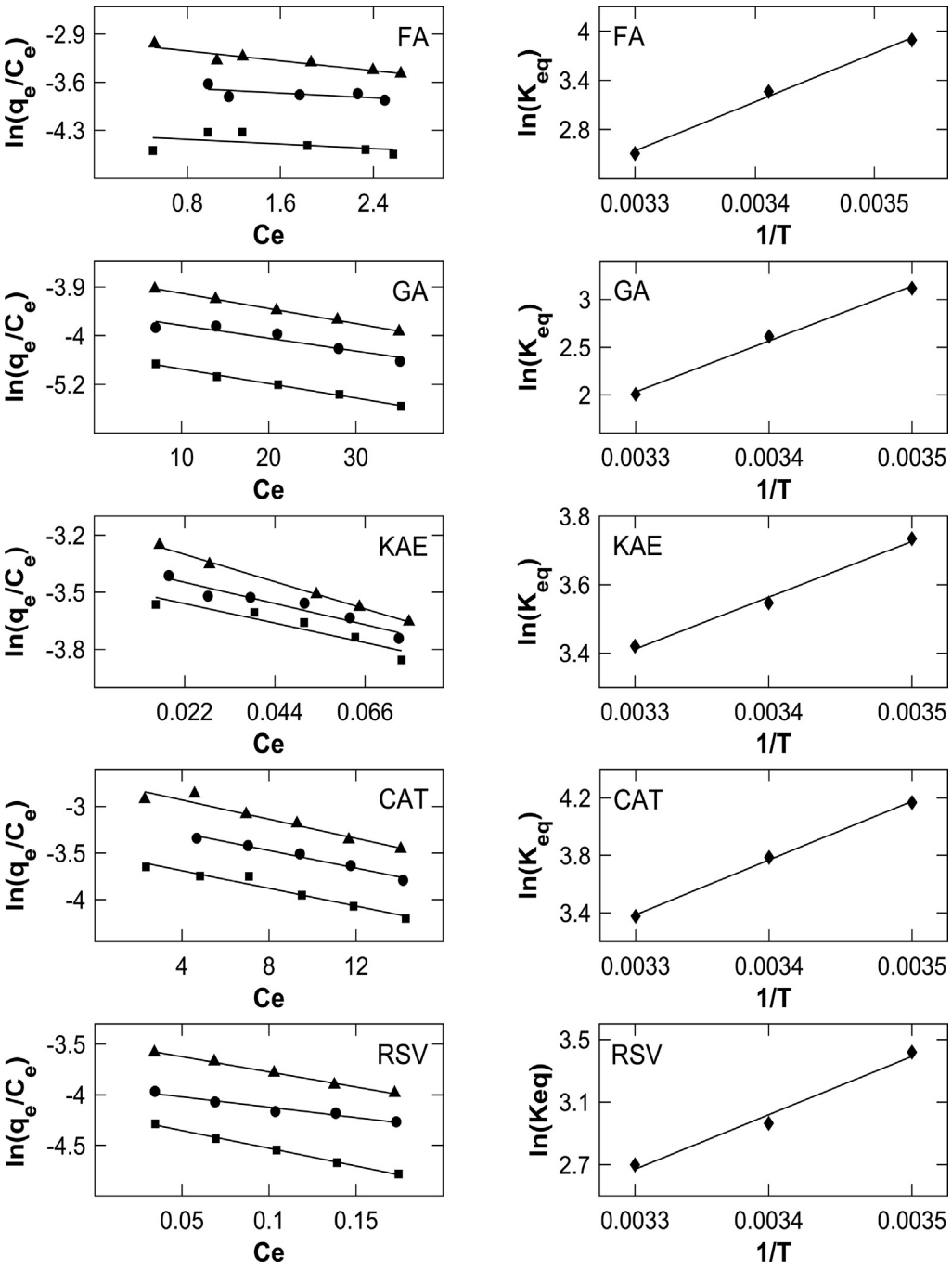

Fig. 5. Plots of $\ln(q_e/C_e)$ versus q_e to calculated K_{eq} (left column) and van't Hoff plots (right column) for the five polyphenols (FA, GA, KAE, CAT, and RSV). ▲: 10 °C, ●: 20 °C, and ■: 30 °C.

accurate for FA and KAE isotherms than Langmuir's since *CIs* of Freundlich parameters were significantly smaller. For CAT and RSV, model parameters showed the same trend, but *CIs* of Freundlich model parameters were only slightly smaller in these cases. For GA isotherms, parameter *CIs* of both models were almost the same size. The parameter correlation matrix (|C|) is helpful to identify non-determinable model parameters, i.e., those that are correlated. Most FA and KAE Langmuir isotherms (except two, see Table 3) presented highly correlated parameters ($|C| \geq 0.9934$); therefore, this supports that the Freundlich model represents better the adsorption of these two polyphenols on agarose. Similarly, Freundlich represents the RSV isotherms better since Langmuir contains highly correlated parameters in two isotherms, and the |*C*| Langmuir values were larger than Freundlich in five isotherms. Langmuir is the best-fit model for GA and CAT since all isotherm's parameter correlations were lower than Freundlich, which showed highly correlated parameters in three GA isotherms (W100, W94, and W70 at 20 °C).

It is worth mentioning that the overall difference between the two models was not evident with our data; hence, both can be used to represent the isothermal adsorption of the studied polyphenols on agarose adequately. Previous studies have also shown good agreement between these two models and specific equilibrium data [62–64].

Table 4
Thermodynamic parameters for the adsorption of five polyphenols on agarose.

Compound	T (°C)	$K_{eq} \pm U$	$\Delta G \pm U$(kJ/mol)	$\Delta H \pm U$ (kJ/mol)	$\Delta S \pm U$(J/mol K)	R^2
FA	10	49.0 ± 2.7	−9.16 ± 0.13	−49.3 ± 4.4	−141 ± 15	0.9947
	20	26.2 ± 2.8	−7.96 ± 0.26			
	30	12.3 ± 1.6	−6.32 ± 0.34			
GA	10	22.59 ± 0.20	−7.339 ± 0.021	−39.6 ± 2.9	−114 ± 10	0.9945
	20	13.7 ± 1.2	−6.37 ± 0.21			
	30	7.44 ± 0.16	−5.058 ± 0.055			
KAE	10	41.87 ± 0.42	−8.792 ± 0.024	−11.2 ± 1.1	−8.7 ± 3.6	0.9913
	20	34.7 ± 1.2	−8.643 ± 0.088			
	30	30.6 ± 1.6	−8.62 ± 0.13			
CAT	10	64.6 ± 3.9	−9.81 ± 0.14	−28.2 ± 1.1	−64.8 ± 3.7	0.9985
	20	44.1 ± 1.8	−9.23 ± 0.10			
	30	29.3 ± 1.3	−8.51 ± 0.12			
RSV	10	30.54 ± 0.35	−8.049 ± 0.027	−25.7 ± 3.4	−63 ± 12	0.9826
	20	19.37 ± 0.56	−7.224 ± 0.070			
	30	14.87 ± 0.18	−6.804 ± 0.030			

The n parameter values in the Freundlich model can indicate whether the adsorption is irreversible ($10 < n$), very favorable ($2 < n < 10$), moderately favorable ($1 < n < 2$) and unfavorable ($n < 1$) [33,65]. In most cases, the five polyphenols had moderately favorable adsorptions. A few cases showed very favorable adsorption (n higher than 2 with $n_{max} = 2.979$). Moderate adsorptions are suitable for chromatography, where analytes should be retained momentarily to achieve differentiated elution. In addition, n inverse value in the range 0–1 is a measure of adsorbent surface heterogeneity, being more heterogeneous as n inverse value gets closer to zero [47,66]. Therefore, the agarose surface exhibited a slight heterogeneity in all cases because n inverse values were far from zero ($1/n > 0.5$ for most cases and $1/n > 0.35$ only for 9 of 33 cases). The adsorption capacities (K_F) and the maximum adsorption capacities (q_{max}) of all the well-fitted Langmuir models decreased with ethanol and acetic acid, verifying that adsorption is higher when the liquid phase has greater water proportion, as previously discussed. These isothermal equilibrium parameters provide information on the type of polyphenol-agarose-liquid phase interactions. They can also be used to develop first-principles models to optimize and scale-up APLC systems.

3.3. Thermodynamic analysis

Adsorption experiments of the five polyphenols on agarose using the W70 liquid phase (70:15:15 v/v, H_2O:EtOH:HAc) were performed at three different temperatures: 10, 20, and 30 °C (Fig. 4). For all the evaluated polyphenols, the adsorption was reduced with increasing temperature, confirming the exothermic characteristic of the adsorption process. This behavior was expected since almost any adsorption process is exothermic, where the total energy released at the adsorbent-adsorbate junction is larger than the total energy absorbed by bond breakage [67]. An increase in 10 °C (from 10 to 20 °C) reduces the average percentual adsorptions of the five polyphenols. FA was the most affected with a reduction of 34.8%, followed by GA, RSV, and CAT with similar adsorption reductions equal to 29.6%, 28.8%, 28.6%, respectively; KAE was the least affected (7.0%). Similarly, an increment of 20 °C (10 to 30 °C) reduced the average adsorptions by 67.1% for FA > 65.5% for GA > 57.7% for RSV > 51.6% for CAT > 17.9% for KAE.

The enthalpy (ΔH) and entropy (ΔS) of adsorption were determined from Fig. 5, whose values are summarized together with the Gibbs energy (ΔG) values (calculated from Eq. (10)) in Table 4. The isosteric enthalpy (ΔH_x) of adsorption was computed from Fig. 6 and is shown in Table 5. All these thermodynamic parameters appear with their respective combined standard uncertainty. For all cases, the negative values of ΔH suggest that the adsorption processes were exothermic and that an increase in temperature hindered the adsorption process. The $|\Delta H|$ value also indicates if the process is ruled by chemisorption (80–200 kJ/mol) or physisorption (2.1–20.9 kJ/mol) [67]. KAE adsorption was the only process completely ruled by physisorption, which makes KAE-agarose binding interactions relatively weak. Additionally, KAE was the polyphenol with less affinity towards agarose among the five studied polyphenols. The adsorption enthalpies of FA, GA, CAT, and RSV, were higher than the values established for physisorption and lower than those for chemisorption, then these can be attributed to a physicochemical adsorption process. This idea is supported by the fact that hydrogen bonding energy (physisorption) is usually in the range of 8 – 50 kJ/mol [63], and cross-linked 12% agarose provides many hydrogen bonds acceptor sites for the polyphenol's hydroxyl groups. Hence, hydrogen bonding has been established as the dominant adsorption factor in polyphenol-agarose systems [58,60]. Hence, no structural changes occurred on agarose, and no desorption limitations were involved [32]. In the adsorption of FA and GA (both with the highest absolute values of enthalpy, see Table 4), multiple hydrogen bonding FA-agarose and GA-agarose could have been involved [63]. Furthermore, since hydrogen bonding energy strongly depends on the distance of the atoms involved [68], it may also be possible that the hydrogen bonds formed by FA and GA with agarose are much closer to the surface than those formed by KAE, CAT, or RSV. The $|\Delta H_x|$ value (Table 5) corroborated that FA, GA, CAT, and RSV adsorptions were not ruled by chemisorption since $|\Delta H_x|$ values lower than 80 kJ/mol were established for physisorption and $|\Delta H_x|$ values between 80 and 400 kJ/mol indicate the possible presence of chemisorption [53]. In addition, according to the variation of $|\Delta H_x|$ with the surface coverage (adsorption capacity) (Table 5), the degree of heterogeneity of the adsorbent surface can be confirmed, while a constant value of $|\Delta H_x|$ would indicate a homogeneous surface [67,69]. In this study, a slight degree of heterogeneity of the agarose surface can be attributed because the variation of $|\Delta H_x|$ was moderate in all cases, which agreed with that indicated by the isothermal parameter n.

Negative values of ΔG (Table 4) indicate that the adsorption process was spontaneous and thermodynamically feasible for all the studied cases [67]. Polyphenol's adsorption was more spontaneous and more favorable energetically at lower temperatures. Negative values of ΔS, for all cases studied, indicate that polyphenol molecules were organized less randomly (more ordered) at the polyphenol-agarose interface during the adsorption process ($\Delta S < 0$ means less random and $\Delta S > 0$ means more random) [67,70]. $|\Delta S|$ value of KAE adsorption was lower than those of CAT and RSV adsorption and much lower than those of phenolic acids adsorption (FA and GA). It could be speculated that the lower $|\Delta S|$ of KAE is related to the higher –OH moieties of KAE, in which

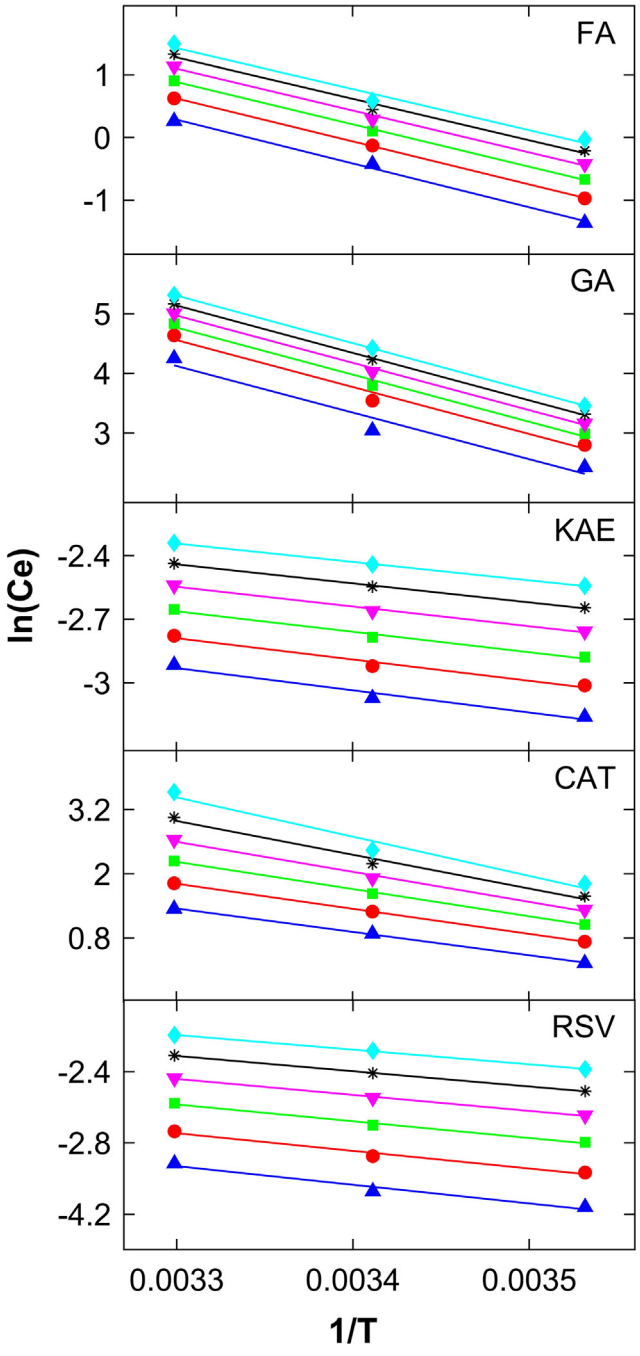

Fig. 6. Plots of ln(C_e) versus *1/T* for adsorptions of FA, GA, KAE, CAT, and RSV on agarose. ▲, ●, ■,▼, *, and ◆ represent the six constant adsorbed amounts (q) defined in the concentration range of each polyphenol (Table 5).

more spatial configurations are available for the adsorption of this compound on the surface. Hence, the order of the system does not change as much as when only one or two spatial configurations are available (as in the case of the phenolic acids).

R^2 is the coefficient of determination of the van't Hoff plot, and U is the combined standard uncertainly.

3.4. Three-component mixing experiments in APLC system

According to the adsorption values calculated for the five polyphenols independently in a batch system, the order of elution of the fractions from an APLC system could be established as

Table 5
The isosteric adsorption enthalpy change of five polyphenols on agarose.

Compound	q (mmol/g)	$\Delta H_x \pm U$(kJ/mol)	R^2
FA	1.5E-02	−58.06 ± 4.01	0.9953
	2.0E-02	−56.98 ± 0.73	0.9998
	2.5E-02	−56.1 ± 1.8	0.9990
	3.0E-02	−55.5 ± 3.9	0.9951
	3.5E-02	−54.9 ± 5.6	0.9895
	4.0E-02	−54.4 ± 7.2	0.9829
GA	2.0E-01	−64.9 ± 9.5	0.9585
	2.5E-01	−65.4 ± 8.5	0.9832
	2.8E-01	−65.6 ± 6.1	0.9917
	3.1E-01	−65.9 ± 3.8	0.9968
	3.4E-01	−66.1 ± 1.7	0.9993
	3.7E-01	−66.25 ± 0.18	1.0000
KAE	1.3E-03	−8.7 ± 1.6	0.9680
	1.5E-03	−8.3 ± 1.2	0.9785
	1.6E-03	−8.02 ± 0.93	0.9869
	1.8E-03	−7.73 ± 0.64	0.9931
	1.9E-03	−7.46 ± 0.38	0.9974
	2.1E-03	−7.21 ± 0.14	0.9996
CAT	1.0E-01	−36.3 ± 1.1	0.9991
	1.4E-01	−38.96 ± 0.11	1.0000
	1.8E-01	−42.3 ± 1.6	0.9986
	2.2E-01	−46.6 ± 3.5	0.9943
	2.6E-01	−52.5 ± 6.3	0.9857
	3.0E-01	−61.0 ± 9.8	0.9711
RSV	1.3E-03	−8.7 ± 1.6	0.9680
	1.5E-03	−8.2 ± 1.1	0.9815
	1.7E-03	−7.82 ± 0.73	0.9913
	1.9E-03	−7.46 ± 0.38	0.9974
	2.1E-03	−7.13 ± 0.11	0.9999
	2.3E-03	−6.84 ± 0.22	0.9990

KAE < GA < FA < CAT < RSV (elution times). These results also suggest that the elutions of the five polyphenols are feasible and favorable for the APLC system with Superose™ 12-H_2O:EtOH:HAc phases. Only RSV would present a more significant delay in its elution according to its high percentage of average adsorption calculated. Therefore its elution can be accelerated with the addition of EtOH:HAc to the mobile phase. Based on these assertions and corroborating them, an aqueous mixture of GA, CAT, and RSV was fractionated in an APLC system with Superose™ 12 as the stationary phase and the liquid mixtures W94 and W70 as mobile phases. The fractions eluted from the APLC system in the same order (GA < CAT < RSV) suggested by the adsorption analysis in batch system of individual polyphenols (Fig. 7, left and right). It was also evidenced that resveratrol had a significantly higher delay than the other polyphenols studied, especially for the mobile phase with higher water content (Fig. 7, left). According to the adsorption equilibrium analysis in the batch system, the mobile phase composition affects the studied polyphenols differently. In the APLC system, it could be seen that the change from W94 to W70 accelerates the elution of GA in ~ 4 min, CAT in ~ 9 min, and RSV in ~ 39 min. This difference can be used to find the optimal path of the mobile phase gradient applying a predictive mathematical model. This optimization can accelerate the elution of RSV while maintaining the high resolution of the other fractions (GA and CAT).

4. Conclusions

Adsorption of five relevant low molecular weight polyphenols on Superose™ 12 prep grade from liquid phases with different compositions (H_2O:EtOH:HAc) was explored and characterized. Each polyphenol was independently evaluated with three or six liquid phases to simulate the different mobile phases used in isocratic and gradient APLCs. Fitting experimental values to standard isotherm models (Langmuir and Freundlich) allowed estimating significant and uncorrelated parameters for 33 different cases.

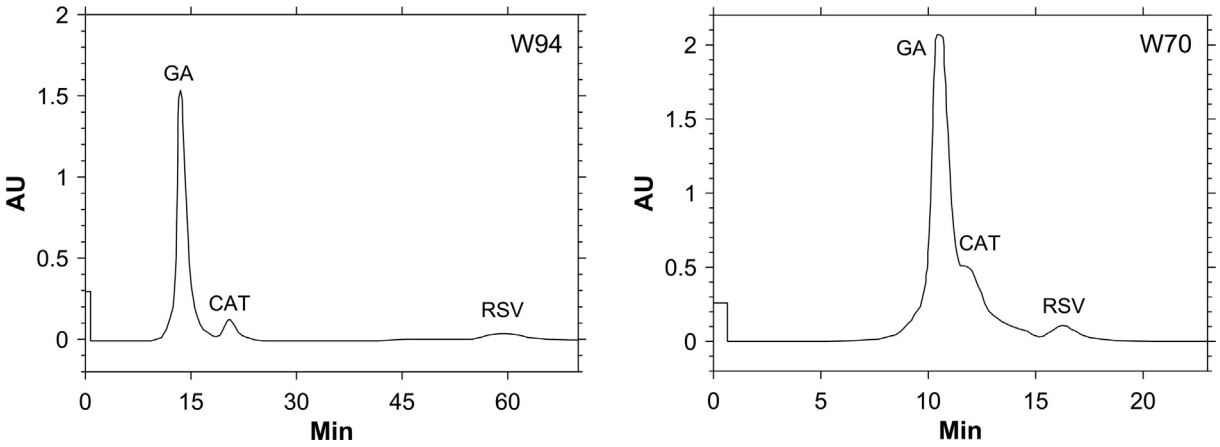

Fig. 7. Isocratic adsorption chromatography of a mixture of gallic acid, catechin, and resveratrol on Superose™ 12 column. Mobile phase: 3% ethanol, 3% acetic acid, 94% water (W94, left); and 15% ethanol, 15% acetic acid, 70% water (W70, right).

These parameters, which have not been reported, are essential input data for developing predictive theoretical models of the APLC system.

Isotherms' form (L-type) indicated that probably all these polyphenols are horizontally adsorbed, there is no significant competition with the liquid phase, and as the sites in agarose are filled, adsorption becomes more difficult. Different affinities of the polyphenols with agarose were observed.

Polyphenols had different affinities for Superose™ 12, which is favorable for isolating these compounds by APLC. The hypothetical elution order (GA < CAT < RSV) determined from the adsorption analysis was corroborated with experiments in an APLC system. Lowering the water proportion or increasing the EtOH:HAc proportion in the liquid phase reduced the adsorption of the studied polyphenols. The same effect had the increase in temperature. This reduction was different for each polyphenol, which can accelerate the elution of RSV without impairing the resolution of CAT and GA in the APLC process. The W30 mixture reduces the adsorption of four polyphenols (except FA) up to $\sim$ 0.9%; hence, this mobile phase can be used in the last elution step in gradient APLC to accelerate the elution of all fractions that were already separated.

The goodness of fit statistics (R^2 and S) indicated that both isotherm models were adequate and fitted all experimental curves correctly. However, the statistics referring to the parameters (CC, CI, C), especially C, indicated that the Freundlich model represented better FA, KAE, and RSV adsorptions, while the Langmuir model was better for GA and CAT. It should be mentioned that the differences between models were not significant in some cases.

The thermodynamic analysis indicated that the adsorption processes were exothermic (negative values of ΔH), spontaneous, thermodynamically feasible ($\Delta G < 0$), and governed by physisorption. In addition, the adsorbed polyphenols were less randomly organized (more ordered) than those in solution ($\Delta S < 0$). This characterization reaffirms that the Superose™ 12 is a suitable stationary phase to fractionate polyphenols in an APLC system.

CRediT authorship contribution statement

Pamela Raquel Rivera-Tovar: Data curation, Formal analysis, Investigation, Methodology, Software, Writing – original draft, Visualization. **Javiera Pérez-Manríquez:** Data curation, Formal analysis, Investigation, Methodology, Software, Writing – original draft, Visualization, Validation. **María Salomé Mariotti-Celis:** Supervision, Writing – review & editing. **Néstor Escalona:** Conceptualization, Writing – review & editing. **José Ricardo Pérez-Correa:** Conceptualization, Supervision, Writing – review & editing, Validation.

Declaration of Competing Interest

The authors declare that they have no known competing financial interests or personal relationships that could have appeared to influence the work reported in this paper.

Acknowledgments

Financial support from FONDECYT Regular project number 1180571. We appreciate the text edition by Lisa Gingles and the support in carrying out many adsorption experiments by Carlos Ybañez and Bruno González. The APLC experiments were carried out by PR at the laboratory of prof. Herminia Domínguez at the Department of Chemical Engineering, Campus Ourense, Universidade de Vigo, Spain.

Appendix A. Supplementary material

Supplementary data to this article can be found online at https://doi.org/10.1016/j.molliq.2021.117972.

References

[1] A. Sławińska-Brych, B. Zdzisińska, M. Dmoszyńska-Graniczka, W. Jeleniewicz, J. Kurzepa, M. Gagoś, A. Stepulak, Xanthohumol inhibits the extracellular signal regulated kinase (ERK) signalling pathway and suppresses cell growth of lung adenocarcinoma cells, Toxicol. 357 (2016) 65–73, https://doi.org/10.1016/j.tox.2016.06.008.

[2] G. Chiva-Blanch, S. Arranz, R.M. Lamuela-Raventos, R. Estruch, Effects of wine, alcohol and polyphenols on cardiovascular disease risk factors: evidences from human studies, Alcohol Alcoholism. 48 (2013) 270–277, https://doi.org/10.1093/alcalc/agt007.

[3] H. Kanno, Z. Kawakami, M. Tabuchi, K. Mizoguchi, Y. Ikarashi, Y. Kase, Protective effects of glycycoumarin and procyanidin B1, active components of traditional Japanese medicine yokukansan, on amyloid β oligomer-induced neuronal death, J. Ethnopharmacol. 159 (2015) 122–128, https://doi.org/10.1016/j.jep.2014.10.058.

[4] H. Yang, L. Xiao, Y. Yuan, X. Luo, M. Jiang, J. Ni, N. Wang, Procyanidin B2 inhibits NLRP3 inflammasome activation in human vascular endothelial cells, Biochem. Pharmacol. 92 (4) (2014) 599–606, https://doi.org/10.1016/j.bcp.2014.10.001.

[5] M. Suganuma, A. Takahashi, T. Watanabe, K. Iida, T. Matsuzaki, H.Y. Yoshikawa, H. Fujiki, Biophysical approach to mechanisms of cancer prevention and treatment with green tea catechins, Mol. 21 (2016) 1566, https://doi.org/10.3390/molecules21111566.

[6] J. Zhu, H. Tang, Z. Zhang, Y. Zhang, C. Qiu, L. Zhang, P. Huang, F. Li, Kaempferol slows intervertebral disc degeneration by modifying LPS-induced osteogenesis/adipogenesis imbalance and inflammation response in BMSCs, Int. Immunopharmacol. 43 (2017) 236–242, https://doi.org/10.1016/j.intimp.2016.12.020.

[7] R. Harini, K.V. Pugalendi, Antihyperglycemic effect of protocatechuic acid on streptozotocin-diabetic rats, J. Basic Clin. Physiol. Pharmacol. 21 (2010) 79–92, https://doi.org/10.1515/JBCPP.2010.21.1.79.
[8] M. Jang, L. Cai, G.O. Udeani, K.V. Slowing, C.F. Thomas, C.W.W. Beecher, H.H.S. Fong, N.R. Farnsworth, A.D. Kinghorn, R.G. Mehta, R.C. Moon, J.M. Pezzuto, Cancer chemopreventive activity of resveratrol, a natural product derived from grapes, Sci. 275 (5297) (1997) 218–220, https://doi.org/10.1126/science:275.5297.218.
[9] S. Garvin, K. Öllinger, C. Dabrosin, Resveratrol induces apoptosis and inhibits angiogenesis in human breast cancer xenografts in vivo, Cancer Lett. 231 (1) (2006) 113–122, https://doi.org/10.1016/j.canlet.2005.01.031.
[10] S. Mandel, M.B.H. Youdim, Catechin polyphenols: neurodegeneration and neuroprotection in neurodegenerative diseases, Free Radic. Biol. Med. 37 (3) (2004) 304–317, https://doi.org/10.1016/j.freeradbiomed.2004.04.012.
[11] S.A. Heleno, A. Martins, M.J.R. Queiroz, I.C. Ferreira, Bioactivity of phenolic acids: Metabolites versus parent compounds: A review, Food Chem. 173 (2015) 501–513, https://doi.org/10.1016/j.foodchem.2014.10.057.
[12] P.R. Rivera-Tovar, M.D. Torres, C. Camilo, M.S. Mariotti-Celis, H. Domínguez, J. R. Pérez-Correa, Multi-response optimal hot pressurized liquid recovery of extractable polyphenols from leaves of maqui (Aristotelia chilensis [Mol.] Stuntz), Food Chem. 357 (2021) 129729, https://doi.org/10.1016/j.foodchem.2021.129729.
[13] N.L. Huaman-Castilla, M. Martínez-Cifuentes, C. Camilo, F. Pedreschi, M. Mariotti-Celis, J.R. Pérez-Correa, The impact of temperature and ethanol concentration on the global recovery of specific polyphenols in an integrated HPLE/RP process on Carménère pomace extracts, Mol. 24 (2019) 3145-, https://doi.org/10.3390/molecules24173145.
[14] M.S. Mariotti-Celis, M. Martínez-Cifuentes, N. Huamán-Castilla, M. Vargas-González, F. Pedreschi, J.R. Pérez-Correa, The antioxidant and safety properties of spent coffee ground extracts impacted by the combined hot pressurized liquid extraction–resin purification process, Mol. 23 (2018) 21, https://doi.org/10.3390/molecules23010021.
[15] L. Barbosa-Pereira, A. Bilbao, P. Vilches, I. Angulo, J. Lluis, B. Fité, P. Paseiro-Losada, J.M. Cruz, Brewery waste as a potential source of phenolic compounds: Optimisation of the extraction process and evaluation of antioxidant and antimicrobial activities, Food Chem. 145 (2014) 191–197, https://doi.org/10.1016/j.foodchem.2013.08.033.
[16] V. Neveu, J. Perez-Jiménez, F. Vos, V. Crespy, L. du Chaffaut, L. Mennen, C. Knox, R. Eisner, J. Cruz, D. Wishart, A. Scalbert, Phenol-Explorer: an online comprehensive database on polyphenol contents in foods., (2010). https://doi.org/10.1093/database/bap024
[17] N. Mirabella, V. Castellani, S. Sala, Current options for the valorization of food manufacturing waste: a review, J. Clean. Prod. 65 (2014) 28–41, https://doi.org/10.1016/j.jclepro.2013.10.051.
[18] J.D. Reber, D.L. Eggett, T.L. Parker, Antioxidant capacity interactions and a chemical/structural model of phenolic compounds found in strawberries, Int. J. Food Sci. Nutr. 62 (5) (2011) 445–452, https://doi.org/10.3109/09637486.2010.549115.
[19] J. Valls, S. Millán, M.P. Martí, E. Borràs, L. Arola, Advanced separation methods of food anthocyanins, isoflavones and flavanols, J. Chromatogr. A. 1216 (43) (2009) 7143–7172, https://doi.org/10.1016/j.chroma.2009.07.030.
[20] M. Gu, Z.-G. Su, J.-C. Janson, The separation of polyphenols by isocratic hydrogen bond adsorption chromatography on a cross-linked 12% agarose gel, Chromatogr. 64 (5-6) (2006) 247–253, https://doi.org/10.1365/s10337-006-0039-z.
[21] D. Liu, Y. Ma, Y.e. Wang, Z. Su, M. Gu, J.-C. Janson, One-step separation and purification of hydrolysable tannins from Geranium wilfordii Maxim by adsorption chromatography on cross-linked 12% agarose gel, J. Sep. Sci. 34 (9) (2011) 995–998, https://doi.org/10.1002/jssc.201100006.
[22] M. Gu, Z.-G. Su, J.-C. Janson, One-step purification of 3, 4-dihydroxyphenyllactic acid, salvianolic acid B, and protocatechualdehyde from Salvia miltiorrhiza Bunge by isocratic stepwise hydrogen bond adsorption chromatography on cross-linked 12% agarose, J. Chromatogr. Sci. 46 (2) (2008) 165–168.
[23] M. Gu, Z.G. Su, J.C. Janson, One-step purification of resveratrol and polydatin from Polygonum cuspidatum (Sieb. & Zucc.) by isocratic hydrogen bond adsorption chromatography on cross-linked 12% agarose, Chromatogr. 64 (2006) 701–704, https://doi.org/10.1365/s10337-006-0081-x.
[24] J. Xu, T. Tan, J.-C. Janson, One-step purification of epigallocatechin gallate from crude green tea extracts by mixed-mode adsorption chromatography on highly cross-linked agarose media, J. Chromatogr. A. 1169 (1-2) (2007) 235–238, https://doi.org/10.1016/j.chroma.2007.08.085.
[25] T. Gu, Parameter estimation and mass transfer effects in liquid chromatography simulation, in: Mathematical Modeling and Scale-Up of Liquid Chromatography With Application Examples, Second, Springer Int. Publ. Switzerland, 2015: pp. 39–62.
[26] G. Guiochon, A. Felinger, D.G. Shirazi, A.M. Katti, Single-component equilibrium isotherms and Competitive equilibrium isotherms, in: Fundamentals of Preparative and Nonlinear Chromatography, Second, Elsevier Inc., San Diego, USA, 2006: pp. 70–214.
[27] G. Guiochon, A. Felinger, D.G. Shirazi, A. Katti, The mass balance equation of chromatography and its general properties, in: Fundamentals of Preparative and Nonlinear Chromatography, Second, Elsevier Inc, San Diego, USA, 2006, pp. 21–63.
[28] A. Tarafder, Modeling and multi-objective optimization of a chromatographic system, in: G. Pandu, A. Bonilla-Petriciolet (Eds.), Multi-Objective Optimization in Chemical Engineering: Developments and Applications, John Wiley & Sons Ltd, First, 2013, pp. 370–397.
[29] I. Langmuir, The adsorption of gases on plane surfaces of glass, mica and platinum, J. Am. Chem. Soc. 40 (9) (1918) 1361–1403.
[30] H. Freundlich, Über die adsorption in lösungen, Zeitschrift Für Physikalische Chemie 57U (1) (1907) 385–470.
[31] H. Motulsky, A. Christopoulos, Fitting models to biological data using linear and nonlinear regression: a practical guide to curve fitting, 2004. www.graphpad.com.
[32] Z.P. Gao, Z.F. Yu, T.L. Yue, S.Y. Quek, Adsorption isotherm, thermodynamics and kinetics studies of polyphenols separation from kiwifruit juice using adsorbent resin, J. Food Eng. 116 (1) (2013) 195–201, https://doi.org/10.1016/j.jfoodeng.2012.10.037.
[33] H.N. Tran, S.-J. You, H.-P. Chao, Thermodynamic parameters of cadmium adsorption onto orange peel calculated from various methods: A comparison study, J. Env. Chem. Eng. 4 (3) (2016) 2671–2682, https://doi.org/10.1016/j.jece:2016.05.009.
[34] J. Cuevas-Valenzuela, Á. González-Rojas, J. Wisniak, A. Apelblat, J.R. Pérez-Correa, Solubility of (+)-catechin in water and water-ethanol mixtures within the temperature range 277.6-331.2K: Fundamental data to design polyphenol extraction processes, Fluid Ph. Equilib. 382 (2015) 279–285, https://doi.org/10.1016/j.fluid.2014.09.013.
[35] N. Haq, N.A. Siddiqui, F. Shakeel, Solubility and molecular interactions of ferulic acid in various (isopropanol + water) mixtures, J. Pharm. Pharmacol. 69 (2017) 1485–1494, https://doi.org/10.1111/jphp.12786.
[36] F. Shakeel, M.M. Salem-Bekhit, N. Haq, N.A. Siddiqui, Solubility and thermodynamics of ferulic acid in different neat solvents: measurement, correlation and molecular interactions, J. Mol. Liq. 236 (2017) 144–150, https://doi.org/10.1016/j.molliq.2017.04.014.
[37] A. Noubigh, M. Abderrabba, E. Provost, Temperature and salt addition effects on the solubility behaviour of some phenolic compounds in water, J. Chem. Thermodyn. 39 (2) (2007) 297–303, https://doi.org/10.1016/j.jct.2006.06.014.
[38] K. Srinivas, J.W. King, L.R. Howard, J.K. Monrad, Solubility of gallic acid, catechin, and protocatechuic acid in subcritical water from (298.75 to 415.85) K, J. Chem. Eng. Data. 55 (9) (2010) 3101–3108, https://doi.org/10.1021/je901097n.
[39] L.-L. Lu, X.-Y. Lu, Solubilities of gallic acid and its esters in water, J. Chem. Eng. Data. 52 (1) (2007) 37–39, https://doi.org/10.1021/je0601661.
[40] T.O. Dabir, V.G. Gaikar, S. Jayaraman, S. Mukherjee, Thermodynamic modeling studies of aqueous solubility of caffeine, gallic acid and their cocrystal in the temperature range of 303 K–363 K, Fluid Ph. Equilib. 456 (2018) 65–76, https://doi.org/10.1016/j.fluid.2017.09.021.
[41] D.R. Telang, A.T. Patil, A.M. Pethe, A.A. Tatode, S. Anand, V.S. Dave, Kaempferol-phospholipid complex: formulation, and evaluation of improved solubility, in vivo bioavailability, and antioxidant potential of kaempferol, J. Excip. Food Chem. 7 (2016) 1174.
[42] K. Zhang, L. Gu, J. Chen, Y. Zhang, Y. Jiang, L. Zhao, K. Bi, X. Chen, Preparation and evaluation of kaempferol-phospholipid complex for pharmacokinetics and bioavailability in SD rats, J. Pharm. Biomed. Anal. 114 (2015) 168–175, https://doi.org/10.1016/j.jpba.2015.05.017.
[43] M. Takanori, W. Isao, U. Hiroshi, Y. Hidekazu, High-efficient chemical preparation of catechinone hair dyestuff by oxidation of (+)-catechin in water/ethanol mixed solution, 繊維学会誌. 70 (2014) 19–22.
[44] E.S. Ha, D.H. Kuk, J.S. Kim, M.S. Kim, Solubility of trans-resveratrol in transcutol HP + water mixtures at different temperatures and its application to fabrication of nanosuspensions, J. Mol. Liq. 281 (2019) 344–351, https://doi.org/10.1016/j.molliq.2019.02.104.
[45] K. Robinson, C. Mock, D. Liang, Pre-formulation studies of resveratrol, Drug Dev. Ind. Pharm. 41 (9) (2015) 1464–1469, https://doi.org/10.3109/03639045.2014.958753.
[46] T.A. Davis, B. Volesky, A. Mucci, A review of the biochemistry of heavy metal biosorption by brown algae, W. Res. 37 (18) (2003) 4311–4330, https://doi.org/10.1016/S0043-1354(03)00293-8.
[47] K.Y. Foo, B.H. Hameed, Insights into the modeling of adsorption isotherm systems, Chem. Eng. J. 156 (1) (2010) 2–10, https://doi.org/10.1016/j.cej.2009.09.013.
[48] B.J. Sánchez, D.C. Soto, H. Jorquera, C.A. Gelmi, J.R. Pérez-Correa, HIPPO: An iterative reparametrization method for identification and calibration of dynamic bioreactor models of complex processes, Ind. Eng. Chem. Res. 53 (48) (2014) 18514–18525, https://doi.org/10.1021/ie501298b.
[49] Z. Wang, S. Peng, M. Peng, Z. She, Q. Yang, T. Huang, Adsorption and desorption characteristics of polyphenols from Eucommia ulmoides Oliv. leaves with macroporous resin and its inhibitory effect on α-amylase and α-glucosidase, Ann. Transl. Med. 8 (2020) 1004, https://doi.org/10.21037/atm-20-5468.
[50] Y. Wu, L. Zhang, J. Mao, S. Liu, J. Huang, Y. You, L. Mei, Kinetic and thermodynamic studies of sulforaphane adsorption on macroporous resin, J. Chromatogr. B Analyt. Technol. Biomed. Life Sci. 1028 (2016) 231–236, https://doi.org/10.1016/j.jchromb.2016.06.035.
[51] M.S. Parada, K. Fernández, Modelling the hydrophilic extraction of the bark of Eucalyptus nitens and Eucalyptus globulus: Adsorption isotherm and thermodynamic studies, Ind. Crop. Prod. 109 (2017) 558–569, https://doi.org/10.1016/j.indcrop.2017.08.059.
[52] S. Milonjic, A consideration of the correct calculation of thermodynamic parameters of adsorption, J. Serbian Chem. Soc. 72 (12) (2007) 1363–1367, https://doi.org/10.2298/JSC0712363M.

[53] P.S. Ghosal, A.K. Gupta, An insight into thermodynamics of adsorptive removal of fluoride by calcined Ca-Al-(NO3) layered double hydroxide, RSC Adv. 5 (128) (2015) 105889–105900, https://doi.org/10.1039/C5RA20538G.
[54] I. Farrance, R. Frenkel, Uncertainty of measurement: a review of the rules for calculating uncertainty components through functional relationships, Clin. Biochem. Rev. 33 (2012) 49.
[55] GE Healthcare -Superose TM, Instructions 52-1782-00 AF. Gel filtration media, 2005. https://gels.yilimart.com/Assets/Images/doc/file/17048901_INSTRUCTION_01.PDF.
[56] C.H. Giles, T.H. MacEwan, S.N. Nakhwa, D. Smith, A system of classification of solution adsorption isotherms, and its use in diagnosis of adsorption mechanisms and in measurement of specific surface areas of solids, J. Chem. Soc. 111 (1960) 3973–3993, https://doi.org/10.1039/jr9600003973.
[57] B. Bai, C. Li, Y. Zhao, Li'an Guo, Y. Shen, One-step separation and purification of resveratrol and polydatin from Polygonum cuspidatum on 20% agarose beads, J. Liq. Chromatogr. Relat. Technol. 37 (19) (2014) 2733–2745, https://doi.org/10.1080/10826076.2013.825864.
[58] T. Tan, Z.-G. Su, M. Gu, J. Xu, J.-C. Janson, Cross-linked agarose for separation of low molecular weight natural products in hydrophilic interaction liquid chromatography, Biotechnol. J. 5 (5) (2010) 505–510, https://doi.org/10.1002/biot.201000017.
[59] E.M. Silva, D.R. Pompeu, Y. Larondelle, H. Rogez, Optimisation of the adsorption of polyphenols from Inga edulis leaves on macroporous resins using an experimental design methodology, Sep. Purif. Technol. 53 (3) (2007) 274–280, https://doi.org/10.1016/j.seppur.2006.07.012.
[60] J. Xu, T. Tan, J.-C. Janson, Mixed-mode retention mechanism for (-)-epigallocatechin gallate on a 12% cross-linked agarose gel media, J. Chromatogr. A. 1137 (1) (2006) 49–55, https://doi.org/10.1016/j.chroma.2006.10.001.
[61] Y. Qi, A. Sun, R. Liu, Z. Meng, H. Xie, Isolation and purification of flavonoid and isoflavonoid compounds from the pericarp of Sophora japonica L. by adsorption chromatography on 12% cross-linked agarose gel media, J. Chromatography A 1140 (1-2) (2007) 219–224, https://doi.org/10.1016/j.chroma.2006.12.002.
[62] N. Qiu, S. Guo, Y. Chang, Study upon kinetic process of apple juice adsorption de-coloration by using adsorbent resin, J. Food Eng. 81 (1) (2007) 243–249, https://doi.org/10.1016/j.jfoodeng.2006.10.030.
[63] J. Huang, K. Huang, S. Liu, Q. Luo, M. Xu, Adsorption properties of tea polyphenols onto three polymeric adsorbents with amide group, J. Coll. Interface Sci. 315 (2) (2007) 407–414, https://doi.org/10.1016/j.jcis.2007.07.005.
[64] M. Ribeiro, D. Silveira, S. Ferreira-Dias, Selective adsorption of limonin and naringin from orange juice to natural and synthetic adsorbents, Eur. Food Res. Technol. 215 (6) (2002) 462–471, https://doi.org/10.1007/s00217-002-0592-0.
[65] O. Hamdaoui, Batch study of liquid-phase adsorption of methylene blue using cedar sawdust and crushed brick, J. Hazard. Mater. 135 (1-3) (2006) 264–273, https://doi.org/10.1016/j.jhazmat.2005.11.062.
[66] F. Haghseresht, G.Q. Lu, Adsorption characteristics of phenolic compounds onto coal-reject-derived adsorbents, Energy and Fuels. 12 (6) (1998) 1100–1107, https://doi.org/10.1021/ef9801165.
[67] P. Saha, S. Chowdhury, Insight into adsorption thermodynamics, in, Thermodynamics (2011) 349–364.
[68] K. Wendler, J. Thar, S. Zahn, B. Kirchner, Estimating the hydrogen bond energy, J. Phys. Chem. A. 114 (35) (2010) 9529–9536, https://doi.org/10.1021/jp103470e.
[69] M.R. Unnithan, T.S. Anirudhan, The kinetics and thermodynamics of sorption of chromium(VI) onto the iron(III) complex of a carboxylated polyacrylamide-grafted sawdust, Ind. Eng. Chem. Res. 40 (12) (2001) 2693–2701, https://doi.org/10.1021/ie0009740.
[70] Y.-H. Li, Z. Di, J. Ding, D. Wu, Z. Luan, Y. Zhu, Adsorption thermodynamic, kinetic and desorption studies of Pb2+ on carbon nanotubes, Water Res. 39 (4) (2005) 605–609, https://doi.org/10.1016/j.watres.2004.11.004.